Chemical Geology 439 (2016) 98–109

Contents lists available at ScienceDirect

Chemical Geology

journal homepage: www.elsevier.com/locate/chemgeo

Oxidative biotransformation of biotite and glauconite by alkaliphilic anaerobes: The effect of Fe oxidation on the weathering of phyllosilicates

Daria G. Zavarzina [a,*], Natalya I. Chistyakova [b], Alexey V. Shapkin [b], Alla V. Savenko [c], Tatyana N. Zhilina [a], Vadim V. Kevbrin [a], Tatiana V. Alekseeva [d], Andrey V. Mardanov [e], Sergey N. Gavrilov [a], Andrey Yu. Bychkov [c]

[a] Winogradsky Institute of Microbiology, Research Center of Biotechnology of the Russian Academy of Sciences, 33, bld. 2 Leninsky Ave., Moscow 119071, Russian Federation
[b] Department of Physics, Lomonosov Moscow state University, Leninskie Gory 1, Moscow 119991, Russian Federation
[c] Department of Geology, Lomonosov Moscow State University, Leninskie Gory 1, 119991, Moscow, Russian Federation
[d] Institute of Physical, Chemical and Biological Problems of Soil Science, Pushchino, Moscow region 142290, Russian Federation
[e] Institute of Bioengineering, Research Center of Biotechnology of the Russian Academy of Sciences, 33, bld. 2 Leninsky Ave., Moscow 119071, Russian Federation

ARTICLE INFO

Article history:
Received 25 February 2016
Received in revised form 14 June 2016
Accepted 15 June 2016
Available online 16 June 2016

Keywords:
Anaerobic iron oxidation
Alkaliphiles
Geoalkalibacter ferrihydriticus
Biotite
Glauconite
Dissimilatory iron reduction
Banded iron formation

ABSTRACT

Two alkaliphilic anaerobic bacteria, namely, the dissimilatory iron-reducer *Geoalkalibacter ferrihydriticus* and the fermentative hydrolytic *Clostridium alkalicellulosi*, along with their co-cultures, are studied to examine their ability to release Si and Fe from two main Fe-containing phyllosilicates in Earth's crust: biotite and glauconite. The formation of magnetically ordered phase(s) within 200 days of incubation was only observed in the presence of *G. ferrihydriticus* whether in a mono- or co-culture but not in the abiotic controls or a pure culture of *C. alkalicellulosi*. The co-culture of these organisms could represent a simple trophic chain in which *C. alkalicellulosi* decomposed microcrystalline cellulose to produce organic acids and ethanol, while *G. ferrihydriticus*, as we expected, utilized these products and reduces Fe(III) in phyllosilicate lattices. Unexpectedly, *G. ferrihydriticus* did not utilize but instead produced an additional 3 mM of acetate during growth with phyllosilicates. An analysis of the Mössbauer spectra of biotite and glauconite that were weathered in the presence of *G. ferrihydriticus* revealed magnetically ordered phases that formed by Fe^{2+} oxidation rather than by Fe^{3+} reduction. The only possible explanation of this phenomenon could be in the ability of *G. ferrihydriticus* to produce acetate during anaerobic Fe^{2+} oxidation with carbonate as an electron acceptor. Thermodynamic calculations show the possibility of such a reaction. Thus, microorganisms with respiratory metabolism could play an active role in the bioweathering of phyllosilicates under alkaline anaerobic conditions. The bacterial anaerobic oxidation of ferrous iron with carbonate as an electron donor is supposed to have played a significant role in ancient environments, serving as one of the causes of banded iron formations.

1. Introduction

Earth's surface rocks are weathered through physical, chemical and biological processes, and their relative effects depend on the environmental conditions (Ferris et al., 1994; Vaughan et al., 2002; Uroz et al., 2009; Gadd, 2010). The interaction between minerals and aqueous fluid on the Earth's surface almost always involves the action of microorganisms and/or their metabolites (Banfield and Nealson, 1998). Microorganisms can participate in mineral dissolution, mineralization, the alteration of mineral surface chemistry, and thus their reactivity (Hutchens, 2009). In particular, mineral dissolution could be accelerated by microbially induced changes in pH and E_h and by the production of organic ligands and siderophores (Grote and Krumbein, 1992; Van Cappellen and Wang, 1996; Kraemer et al., 1999; Liermann et al., 2000; Kalinowski et al., 2000; Gadd, 2010; Melton et al., 2014) or be inhibited by microbial exopolysaccharides, which block reactive centres on the mineral surface (Welch and Vandevivere, 1994; Welch et al., 1999). In addition, carbon dioxide (CO_2) that is released from microbial respiratory processes could cause nonspecific carbonic acid attacks on mineral surfaces (Zavarzina et al., 1996; Ehrlich, 1998; Gadd and Sayer, 2000; Uroz et al., 2009). Several groups of microorganisms, such as dissimilatory iron-reducing bacteria (DIRB), could mobilize metals and attack the surface of minerals through their enzymatic redox activity. These organisms are widespread in nearly all types of natural sedimentary environments (Lovley et al., 2004; Slobodkin, 2005; Roh et al., 2006; Coupland and Johnson, 2008). To date, the physiology and biochemistry of dissimilatory iron reduction has been extensively studied for the representatives of two genera of mesophilic Gram-negative bacteria - *Geobacter* spp. and *Shewanella spp.* (Shi et al., 2007;

* Corresponding author.
E-mail address: zavarzinatwo@mail.ru (D.G. Zavarzina).

http://dx.doi.org/10.1016/j.chemgeo.2016.06.015
0009-2541/

Richter et al., 2012). In the majority of these studies, chemically synthesized ferrihydrite (SF) was utilized as the model mineral source of Fe(III) (Zachara et al., 2002). However, other iron minerals have been reported to serve as electron acceptors for DIRB, namely, oxides and hydroxides (Lovley and Phillips, 1988; Zachara et al., 1998; Bond and Lovley, 2002; Dong et al., 2003; O'Loughlin et al., 2010); silicates; the primarily clay minerals nontronite, illite, and montmorillonite (Dong, 2012; Pentrakova et al., 2013; Zhang et al., 2013; Zhao et al., 2013, 2015; Koo et al., 2014; Liu et al., 2014); and even phyllosilicates (Brookshaw et al., 2014, 2015). All these studies have been performed at neutral pH conditions, and the process of Fe(III) reduction, which is a proton-consuming reaction, becomes less favourable with increasing pH and concomitant decreases in iron solubility (Bethke et al., 2011; Flynn et al., 2014). However, the ability to reduce iron(III) from SF and even phyllosilicates has been documented in alkaliphilic microorganisms that inhabit soda lakes (Gorlenko et al., 2004; Zavarzina et al., 2006, 2011; Pollock et al., 2007; Zhilina et al., 2009a, 2009b, 2015; Chistyakova et al., 2012a, 2012b; Ma et al., 2012; Shapkin et al., 2013; Liu et al., 2015).

Soda lakes are typical natural habitats of alkaliphilic microbial communities. The main mechanism of soda lake formation includes the CO_2–induced leaching of rocks by water, followed by $CaCO_3$ precipitation and sodium carbonate accumulation from evaporation (Zavarzin and Zhilina, 2000). Soda lakes are common terminal basins in hot, arid regions, where silicates rather than carbonate minerals dominate (Eugster and Hardie, 1978). At pH > 9, the bioweathering of minerals could be induced by the excretion of metabolites, while respiratory processes, which lead to carbonic acid attacks on minerals, have minor effects at such environmental conditions.

The goal of this work was to study the ability of alkaliphilic anaerobes to release Si and Fe from two Fe-containing phyllosilicates, specifically, biotite and glauconite, and to identify the prevailing mechanisms of these minerals' bioweathering at high alkalinity. Biotite and glauconite are chosen as the main Fe-bearing minerals in magmatic, metamorphic and sedimentary rocks. Two metabolically different alkaliphilic bacteria are tested for their ability to perform the bioweathering of phyllosilicates at a pH of 9.0. *Clostridium alkalicellulosi* is an alkaliphilic cellulolytic bacterium that degrades cellulose to form ethanol, lactate, formate, acetate and molecular hydrogen as end products (Zhilina et al., 2005). Thus, this organism should influence bioweathering through the production of organic ligands. *Geoalkalibacter ferrihydriticus* is an alkaliphilic DIRB that can reduce iron(III) from SF with acetate, formate, ethanol or lactate as electron donors (Zavarzina et al., 2006, 2011). In binary cultures, these organisms could reproduce a simple trophic chain to decompose complex organic substrates in the anaerobic microbial community of soda lakes. The results of Mössbauer studies on iron(III) reduction from biotite and glauconite by these organisms have previously been published (Chistyakova et al., 2012a, 2012b; Shapkin et al., 2013). Here, we present microbiological, chemical and genomic data to provide a new interpretation of the phenomenon of phyllosilicate bioweathering at high alkalinity.

2. Materials and methods

2.1. Experimental methods

2.1.1. Bacterial strains and minerals

C. alkalicellulosi Z-7026^T (=VKM B-2349 = DSM 17461^T) was isolated from the bottom deposits of the soda lake Verkhnee Beloe (Buryatiya, Russia), which has a pH of 10.2 and mineralization of up to 24.0 g L^{-1} (Zhilina et al., 2005), and *G. ferrihydriticus* Z-0531^T (=VKM B-2349 = DSM 17461^T) was isolated from the bottom deposits of the soda lake Khadyn (Tuva, Russia), which has a water pH of 9.5 and mineralization of 17.0 g L^{-1} (Zavarzina et al., 2006). Selected grains of biotite $(K_{0.89}Na_{0.03})(Mg_{0.9}Fe^{2+}_{1.1}Al_{0.43}Fe^{3+}_{0.22}Ti_{0.09}Mn_{0.03})[Al_{1.26}Si_{2.8}O_{10}](OH,F)_2$ (Karelia, Russia) and glauconite $K_{0.8}(Mg_{0.4}Fe^{2+}_{0.1})(Fe^{3+}_{1.1}Al_{0.4})[(Si_{3.7}Al_{0.3})O_{10}](OH)_2$ (deposit Maardu, Estonia) were crushed into powder <50 μm in an agate mortar. The minerals were not washed before the experiments because their purity was confirmed by X-ray diffractometry, which observed no detectable content of secondary minerals. The chemical composition of both minerals was determined by X-ray fluorescence (XRF) spectroscopy (Table 1). The Fe^{3+}/Fe^{2+} ratios were determined by Mössbauer spectroscopy.

2.1.2. Cultivation conditions

The experiments were performed by using an anaerobically prepared medium with the following composition (g L^{-1}): KH_2PO_4 — 0.2; $MgCl_2$–0.1; NH_4Cl – 0.5; KCl – 0.2; NaCl – 1.0; Na_2CO_3–3.0; $NaHCO_3$–16.0; yeast extract - 0.05; thioglycolate – 0.3; trace element solution (Kevbrin and Zavarzin, 1992) – 1 ml L^{-1}. Microcrystalline cellulose (MCC) Sigmacell 101 (Sigma, US) (1 g L^{-1}) or acetate (1 g L^{-1}) was added as a growth substrate. The pH value of the medium after sterilization was 9.0. This basal medium without bicarbonate, phyllosilicates or MCC was boiled and further cooled down under 100% N_2 flux. Afterward, bicarbonate was added, and the medium was dispensed under N_2 flux by 70-ml portions into 120-ml glass bottles that each contained 200 mg of biotite, glauconite or ferrihydrite (to obtain a final Fe(III) content of 100 mM). The medium was heat sterilized at 120 °C for 30 min. Ferrihydrite (SF) was synthesized by titrating a solution of $FeCl_3 \times 6H_2O$ (60 g L^{-1}, Fulka) with 10% (w/v) NaOH to a pH of 9.0. The obtained mineral was washed three times with distilled water and distributed into the glass bottles. The size of the SF particles was previously verified by Mössbauer spectroscopy, measuring 4.9 ± 1.5 nm (Chistyakova et al., 2012a).

Before the experiments with phyllosilicates, *C. alkalicellulosi* was sustained on the aforementioned medium with MCC as the substrate. *G. ferrihydriticus* was sustained on the same medium, which lacked thioglycolate and contained acetate (1 g L^{-1}) as an electron donor and SF (up to 10 mM of Fe(III)) as an electron acceptor. As *G. ferrihydriticus* colonized the surface of the minerals, the cultures were strongly agitated before transfers, and culture supernatants were used as inocula after the complete precipitation of the solid phase. The cell number of *G. ferrihydriticus* in the supernatants was co. 2.5×10^6 cell ml^{-1}. The media with phyllosilicates were inoculated with *C. alkalicellulosi* (2 vol%), *G. ferrihydriticus* (5 vol%), or both and incubated at 35 °C for 200 days. All the experiments were performed in duplicates. All variants of the experiments and controls are summarized in Table 2.

2.1.3. Analytical methods

Bacterial growth and the concentrations of fermentation products and acetate were monitored during all the incubation periods. The bottles were slightly agitated before sampling. The growth was determined by direct cell counting with a phase contrast light microscope (Reichert Zetopan, Austria). The growth of *G. ferrihydriticus* was also monitored by epifluorescence microscopy with an AxioImager.D1 microscope (Carl Zeiss, Germany) that was equipped with an AxioCamHR digital camera

Table 1
Oxide composition of the phyllosilicates as determined by the XRF method.

	SiO_2	Al_2O_3	FeO[a]	Fe_2O_3[a]	MnO	MgO	CaO	Na_2O	K_2O	TiO_2	P_2O_5	PF	Total
Biotite	*36.4*	19.01	17.3	3.8	0.45	8.0	0.05	0.2	9.3	1.5	<0.01	4.0	100.0
Glauconite	50.9	7.9	5.1	16.2	0.01	3.6	0.6	<0.01	8.3	0.1	0.05	7.2	100.0

[a] Data from Mössbauer spectroscopy.

and relevant filters (Zeiss 20 for Cy3-labeled probes and Zeiss 49 for DAPI-stained cells) by cell staining with acridine orange.

The fermentation products were determined by high-performance liquid chromatography (HPLC) on a Stayer chromatograph (Aquilon, Russia) that was equipped with an Aminex HPX_87H column (Biorad, US) and a Smartline 2300 refractometric detector (Knauer, Germany); 5 mM H_2SO_4 was used as the eluent. The cultures were sampled by using anaerobic techniques with needles and syringes. Samples for chromatography were pre-treated by centrifugation at 12,600*g* on a ELMI CM-50 centrifuge (Latvia) for 3 min, followed by the acidification of the clear supernatant with 5 M H_2SO_4 to a pH of 2.0. The detection limit of the method was 0.2 mM.

The Fe(II) content was determined colorimetrically with ferrozine (Stookey, 1970). The detection limit of the method was 10 μM.

Samples for solid phase analysis were collected at the end of the experiment. The solid phase was separated by centrifugation at 200*g* on a Joan C3i centrifuge (USA) for 5 min and further dried in a desiccator at 35 °C under a 100% N_2 atmosphere over silica gel.

Samples were taken at the end of the experiments and centrifuged as described above, and 50 ml of supernatant was filtered through a 0.22-μm membrane filter to determine the Si content. The silica content was determined colorimetrically with ammonium molybdate and Mohr's salt (Lur'e, 1971). The Si content that transferred from biotite or glauconite was determined according to the following protocol: 40 mg of solid phase was sampled and added to 40 ml of distilled water and then agitated for one month until equilibration, which was judged by approaching a stable concentration of dissolved Si. The equilibrated samples were left to settle mineral particles for the next 2 weeks. Afterward, an optically clear liquid phase was subsampled, filtered and analysed as described above. The detection limit of the method was 1 μM.

The morphology of the minerals was studied by scanning electron microscopy (SEM) by using a TESCAN VEGA 3 LMU device with an INCA Energy 350/X-max 80 energy-dispersive analysis system (OXFORD Instruments NanoAnalysis, UK). Specimens for analyses were pre-fixed with carbon double-sized scotch tape and triply coated with Au.

The mineral composition was studied by using X-ray diffractometry on a Bruker D2 Phaser diffractometer with copper radiation and an Ni filter and by Fourier transform infrared spectroscopy (FTIR) (Nicolet 6700 XT, Thermo Electron Corp.) with the KBr pellet technique. Mössbauer spectroscopy was applied in accordance with the following protocol. Spectra of ^{57}Fe nuclei were recorded in a temperature interval of 4.5–295 K on an MS-1104Em (Research Institute of Physics, Southern Federal University, Russia), which was operated in a constant acceleration mode. Spectral measurements at low temperatures were performed in the SHI-850-5 (Janis Research Co, United States) and MKKMI (TsMII VNIIFTRI, Russia) helium and nitrogen cryostats. The spectrometer was calibrated at room temperature by using standard α-Fe absorbent and a ^{57}Co source in an Rh matrix. The SpectrRelax software was used to process and analyse the Mössbauer spectra (Matsnev and Rusakov, 2014). The magnetic susceptibility (MS) was measured by using a KLY-2 Kappabridge device. Three measurements were made for each sample, which were weighed with a precision of 0.001 g, and normalized mass-specific MS data, which were expressed in $\times 10^{-8}$ m^3 kg^{-1}, were used.

Table 2
Variants of experiments and controls.

	Experiments			Controls		
	Ex1	*Ex2*	*Ex3*	*C1*	*C2*	*C3*
Parameters						
Clostridium alklalicellulosi	+	−	+	−	+	+
Geoalkalibacter ferrihydriticus	−	+	+	−	−	+
MCC (1 g L^{-1})	+	−	+	+	+	+
Acetate (1 g L^{-1})	−	+	−	−	−	−
Biotite/glauconite (200 mg)	+	+	+	+	−	−
SF (100 mM Fe(III) content)	−	−	−	−	−	+
Methods						
Light microscopy	+	+	+	+	+	+
Epifluorescence microscopy	−	+	+	−	−	−
Scanning electron microscopy	+	+	+	−	−	−
High performance liquid chromatography	+	+	+	−	+	+
Fe(II) determination with ferrozine	−	−	−	−	−	+
Si determination with Mohr's salt	+	+	+	+	−	−
Fourier transform infrared spectroscopy	+	+	+	+	−	−
X-ray diffractometry	+	+	+	+	−	−
Mössbauer spectroscopy	+	+	+	+	−	+
Magnetic susceptibility	+	+	+	+	−	−

Designations: (+) presence, (−) absence.

2.2. Thermodynamic calculations

Thermodynamic calculations of the interaction of biotite with aqueous solution were made by using the HCh software (Shvarov, 2015). The 9-component system (H-C-O-Na-Mg-Al-Si-Cl-K-Fe) was selected for calculations. This system consists of a formation of 25 solid phases with permanent composition, biotite solid solution (phlogopite-annite) and aqueous solution with 45 species. Acetate and carbonate were calculated in equilibrium with solid phases. Equilibrium between organic and inorganic carbon was not achieved experimentally because of kinetic limitations, but microorganisms can use this metastable state for life. The calculations were performed under the following experimental conditions: a temperature of 35 °C, a pressure of 1 bar, and the aforementioned culture media and biotite compositions. Water-mineral interactions were simulated by adding small amounts of biotite to the solution (1 mg kg^{-1} in each step), with the calculation steps proportional to the reaction time.

These types of calculations were not performed for glauconite because its thermodynamic data are not defined.

2.3. Genome analysis

Tools from the IMG/ER server (https://img.jgi.doe.gov/cgi-bin/mer/main.cgi) were used for genome analysis. The sequences that were used as templates for specific gene searches are described in the Results section.

3. Results

3.1. Sterile control, C1

Liquid-phase analysis for Si revealed no detectable silica in the sterile controls after 200 days of incubation despite the high pH value. The amount of Si that transferred to the liquid phase from

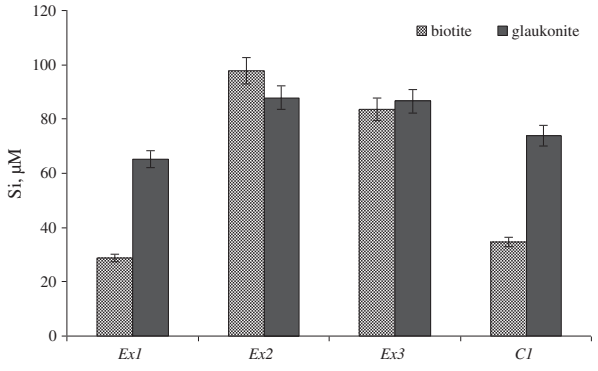

Fig. 1. Changes in the equilibrium concentration of dissolved silica as measured after 200 days of incubation in the experiments (*Ex1–3*) and sterile control (*C1*).

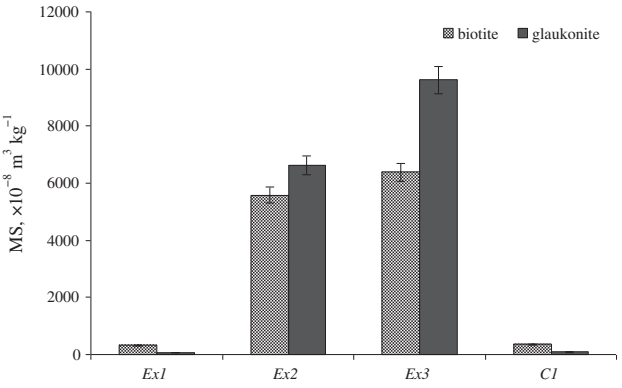

Fig. 2. Changes in the magnetic susceptibility (MS) of the solid phases as measured after 200 days of incubation in the experiments and sterile control.

biotite and glauconite was 34.6 μM and 73.9 μM, respectively (see the last column in Fig. 1). After 200 days of incubation in the sterile control, XRD, FTIR, Mössbauer spectroscopy and MS analyses of phyllosilicates revealed no structural changes in the minerals (Figs. 1, 2, 3, last column bar).)

3.2. Interaction of *Clostridium alkalicellulosi* with phyllosilicates, Ex1, compared to the mineral-free control, C2

The growth of *C. alkalicellulosi* in the presence and absence of minerals began after 5 days of incubation and was accompanied by MCC degradation. After 10 days of incubation, the growth reached a stationary phase. The kinetics of the accumulation of MCC fermentation products in the presence (*Ex1*) and absence (*C2*) of minerals is provided in Fig. 4 and Table 3. The growth rate of *C. alkalicellulosi* was unaffected by the presence of minerals (Fig. 4), but the ratio of fermentation products was influenced by the minerals. In the presence of phyllosilicates, the production of lactate decreased and the acetate concentration increased. The pH after the end of incubation was 8.8 in the experiments with biotite or glauconite and slightly lower (8.7) in the mineral-free control (*C2*). XRD, MS and Mössbauer spectroscopy analyses of the minerals in the cultures correlated with previously published results (Chistyakova et al., 2012b; Shapkin et al., 2013) and did not differ from those from the sterile control (*C1*) (see the first and last column bars in Figs. 1-3, Tables 4,5). However, the FTIR spectra of glauconite revealed a shift in Si-O vibrations from 997 to 1010 cm^{-1}, which could be explained by an increase in the number of swelling layers up to 15% (Manghnani and Hower, 1964). Additionally, several new lines that corresponded to newly formed kaolinite (470, 540, 3619 and

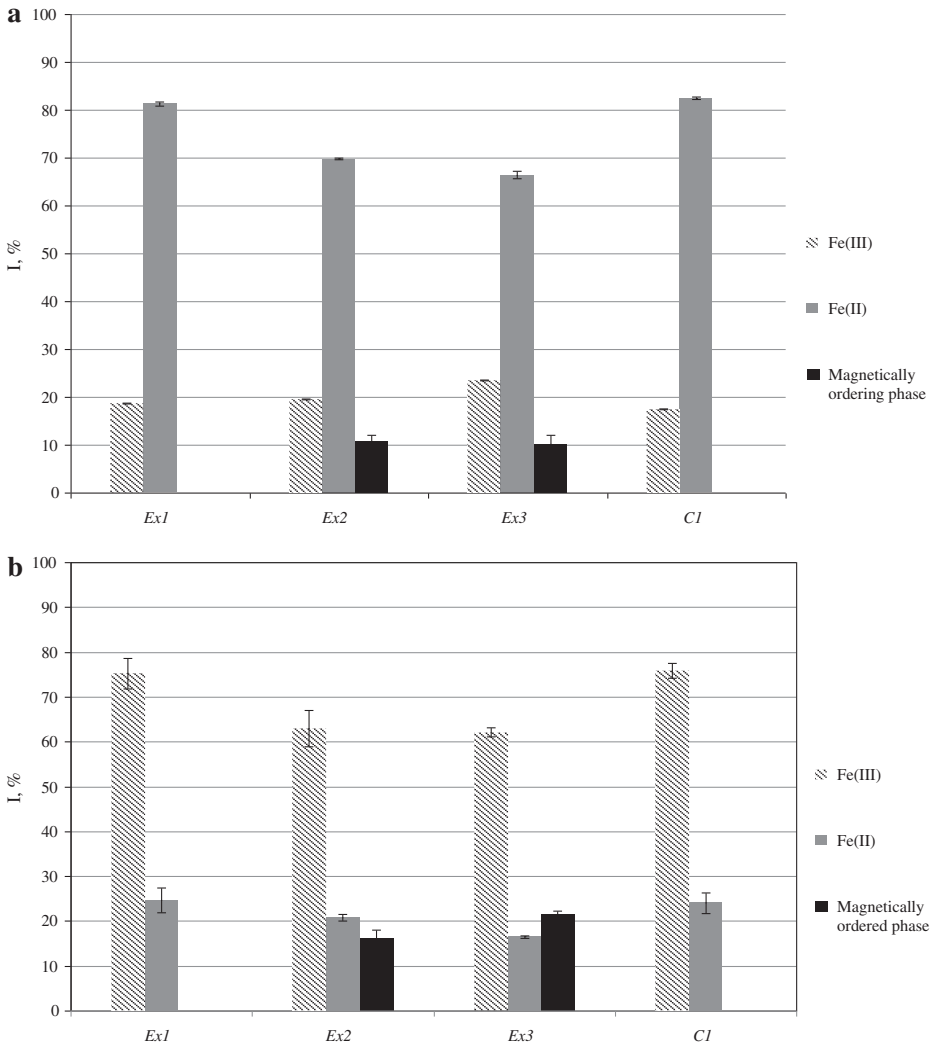

Fig. 3. Total relative intensities of sub-spectra that correspond to Fe^{2+} and Fe^{3+} atoms and magnetically ordered phases in biotite (a) and glauconite (b) as measured after 200 days of incubation in all the experiments (*Ex1–3*) and in the sterile control (*C1*).

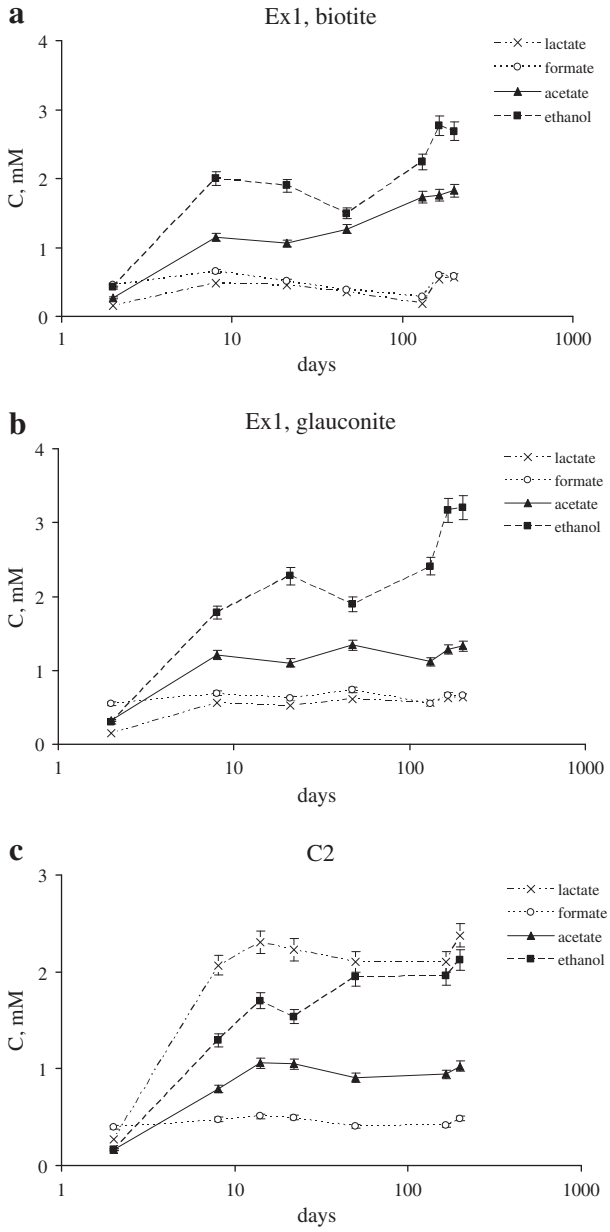

Fig. 4. Formation of liquid fermentation products by *Clostridium alkalicellulosi* during its growth in the presence of biotite (a) and glauconite (b) (*Ex1*) or in the absence of minerals (c) (*C2*). Open circle, formate; filled triangle, acetate; cross, lactate; filled square, ethanol.

3696 cm^{-1}) appeared in the grown cultures. The structure of biotite remained untouched. Silica was not detected in the liquid phase of the grown cultures, and the amount of Si that transferred to the liquid phase from biotite and glauconite was 28.8 and 65.3 μM, respectively, even lower than that in the sterile control (*C1*) (see the first and last column bars in Fig. 1, Table 4).

3.3. Interaction of *Geoalkalibacter ferrihydriticus* with phyllosilicates, Ex2

The number of cells of *G. ferrihydriticus* in culture supernatant during the entire experimental period did not exceed 10^5 cells mL^{-1}. However, epifluorescence microscopy analysis of solid phases, which were stained with acridine orange after the end of the experiment, showed that the cells of *G. ferrihydriticus* were closely associated with minerals and sometimes formed dense colonies (Fig. 5).

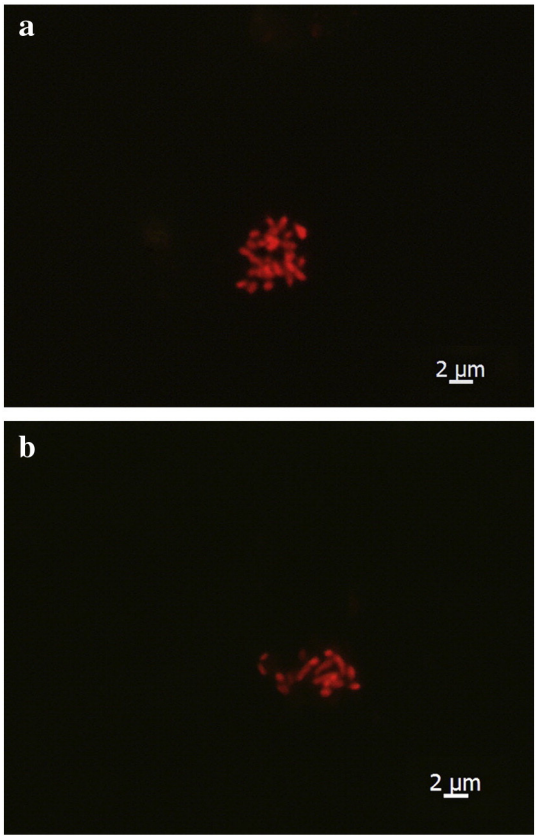

Fig. 5. Epifluorescence micrographs of *Geoalkalibacter ferrihydriticus* cells on the surface of biotite (a) and glauconite (b), which were stained with acridine orange at the end of the experiment.

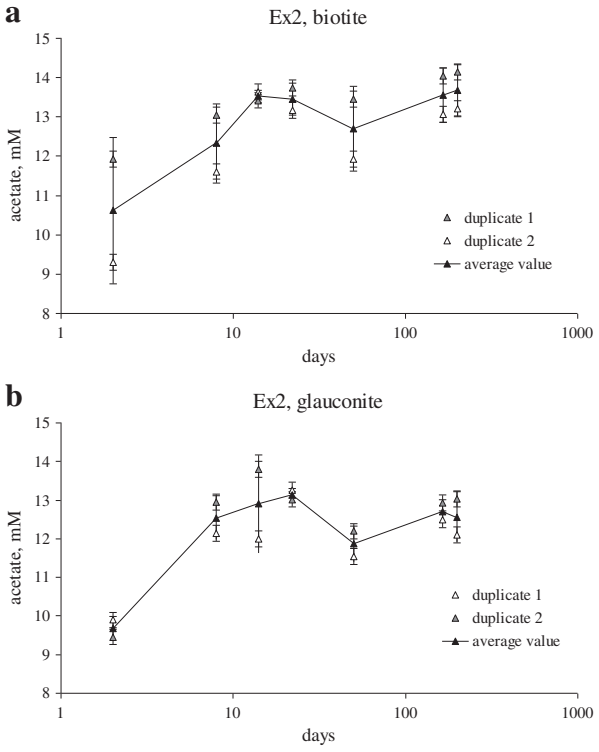

Fig. 6. Acetate concentration that was measured during the growth of *Geoalkalibacter ferrihydriticus* with biotite (a) and glauconite (b). Grey and black triangles, duplicates 1 and 2; line, the average value.

Surprisingly, the concentration of acetate that was added to the medium as a growth substrate did not decrease during the first days of the experiment. Instead, approximately 3 mM was generated with both minerals in both duplicates (Fig. 6, Table 3). After 14 days of incubation, the acetate concentration reached its maximum and stabilized. The pH after the end of the experiment in both duplicates did not change. FTIR spectrometry and XRD analysis data showed that incubation with *G. ferrihydriticus* had little or no apparent effect on the biotite structure. On the contrary, XRD data for glauconite indicated a small but noticeable shift in the (001) peak from 10.112 Å in the sterile control (*C1*) to 10.165 Å in the experiment (*Ex2*). We suppose that these changes were connected to an increase in the number of swelling layers in the glauconite structure. FTIR spectroscopy showed a shift in Si-O vibrations from 997 to 1010 cm^{-1}. This shift confirms the XRD data and corresponds to an increase in swelling layers from 5 to 15% (Manghnani and Hower, 1964).

Mössbauer spectroscopic analysis of biotite and glauconite at the end of the experiment revealed that a novel, magnetically ordered phase formed with both minerals after 200 days of incubation. Previously published spectra that were recorded at 78 K (Chistyakova et al., 2012b; Shapkin et al., 2013) were satisfactorily fit by a superposition of four quadrupole doublets, which corresponded to ferric and ferrous ions in residual biotite and glauconite structures, and one sextet for magnetically ordered phases by using a many-state superparamagnetic relaxation model (Jones and Srivastava, 1986) (Table 5). The relative contents of magnetic phases in biotite and glauconite were 10.7% and 16.2% of the total Fe, respectively (Table 5). An analysis of hyperfine parameters in this sextet showed that the magnetically ordered phases were a mixture of magnetite (Fe_3O_4) and maghemite (γ-Fe_2O_3). According to the relaxation parameter $\alpha = KV/kT$ (*K*– anisotropy energy constant, *V* – particle volume, *k* – Boltzmann's constant, *T* – temperature), the estimated diameter of the magnetically ordered particles was $d \sim 9$ nm (assuming that the particles were spherical). The following constants for magnetite used $K = 1.3 \cdot 104$ J/m^3 for these calculations (Goya et al., 2003). This particle size range and a small magnetically ordered phase content that does not exceed 3% would make this phase undetectable by XRD. Extreme enhancement in the magnetic susceptibility was observed for both minerals: from 320 up to ~6000 $\times$ 10^{-8} m^3 kg^{-1} for biotite and from 60 up to ~8000 $\times$ 10^{-8} m^3 kg^{-1} for glauconite (second column bar in Fig. 2, Table 4). These changes support the formation of a ferrimagnetic phase (magnetite or maghemite) based on the Mössbauer spectroscopy data. As with the *C. alkalicellulosi* experiment, the silica content of the liquid phase in the experiment with *G. ferrihydriticus* was extremely low (≤0.01 mg L^{-1}). However, the concentration of dissolved Si after the end of incubation was 3 times higher in the experiment with biotite (97.7 μM) and nearly 40% higher in the experiment with glauconite (87.9 μM) compared to the experiment with *C. alkalicellulosi* and sterile controls (see the first, second and last column bars in Fig. 1, Table 4).

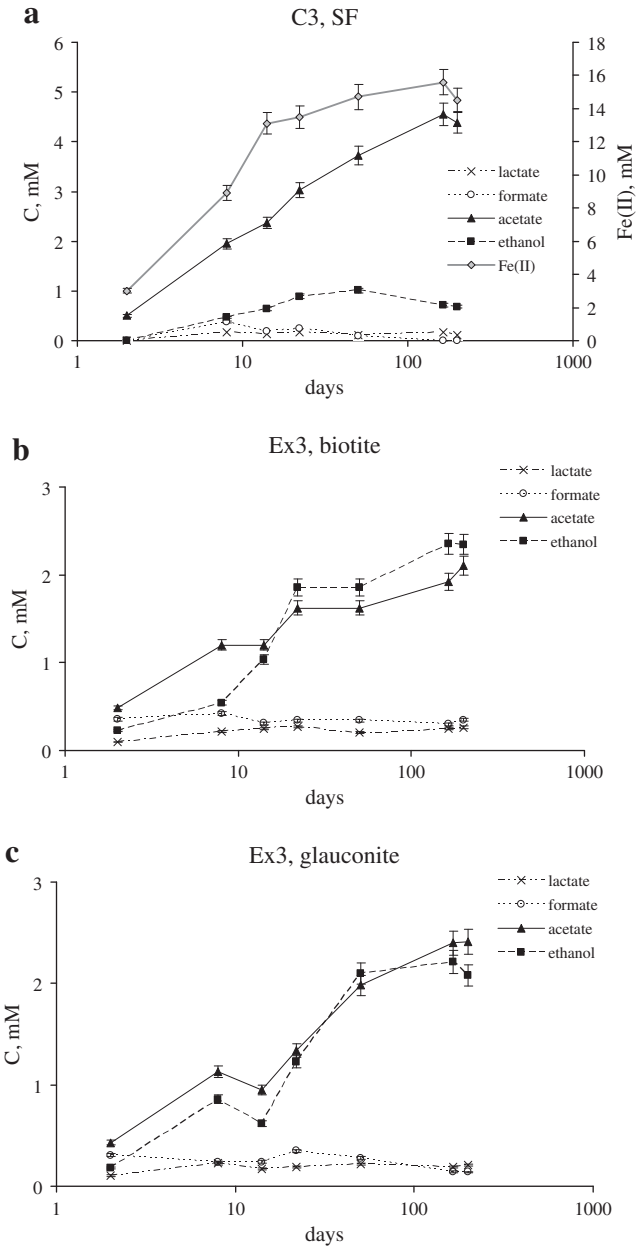

Fig. 7. Growth of *Geoalkalibacter ferrihydriticus* in a co-culture with *Clostridium alkalicellulosi* in the presence of synthesized ferrihydrite (a) (*C3*) or in the presence of biotite (b) or glauconite (c) (*Ex3*). Open circle, formate; filled triangle, acetate; cross, lactate; filled square, ethanol; open rhomb, Fe(II).

3.4. Growth of *C. alkalicellulosi* and *G. ferrihydriticus* co-cultures with minerals

3.4.1. Growth with synthesized ferrihydrite, C3

After 14 days of growth, the colour of the medium became black and magnetic precipitates formed. At the same moment, the concentration of formate that was produced by *C. alkalicellulosi* from MCC began to decrease (Table 3), completely disappearing by the 50th day of the experiment. Afterward, the ethanol concentration began to decrease from ≈1 mM on the 50th day to ≈0.1 mM by the end of the experiment. The acetate content increased during incubation, reaching 4.5 mM by the end of the experiment. On the 14th day of the experiment, the number of *C. alkalicellulosi* and *G. ferrihydriticus* cells in the supernatant reached 7×10^7 and 5×10^6 cells mL^{-1}, respectively, and did not change until the end of the experiment. The final concentration of Fe(II) was 22 mM (Fig. 7a). Mössbauer analysis after the end of the experiment revealed the formation of a mixture of nonstoichiometric magnetite and siderite as products of SF reduction by *G. ferrihydriticus.*

3.4.2. Growth with phyllosilicates, Ex3

The dynamics of the formation of MCC degradation products and the growth of *C. alkalicellulosi* cells in the co-culture on MCC and phyllosilicate minerals are presented in Fig. 7b and c and Table 3. Similarly to *Ex2*, no visible growth of *G. ferrihydriticus* was observed, but its cells were observed by epifluorescence microscopy. The results of solid phase analyses with XRD, FTIR, Mössbauer spectroscopy, MS analysis, SEM and Si dissolution data after the end of the experiment were rather similar to those for the pure culture of *G. ferrihydriticus* (*Ex2*) (see second and third column bars in Fig. 1-3 and Tables 4, 5). However, a comparison of the results of the experiments with *G. ferrihydriticus*

alone and in a co-culture demonstrated that the relative amount of magnetically ordered phases for glauconite in *Ex3* was greater than that in *Ex2*. This amount remained the same for biotite.

3.5. Genome analysis of G. ferrihydriticus

We clearly observed the production of magnetically ordered phases and acetate during the growth of *G. ferrihydriticus* on phyllosilicates but have not yet obtained any direct indications of Fe(III) reduction from biotite or glauconite. We used genome analysis to investigate the ability of *G. ferrihydriticus* to couple acetate production from CO_2 with Fe(II) oxidation to magnetite. We analysed the high-quality draft version of the *G. ferrihydriticus* genome in GenBank under the accession number JWJD00000000 (Badalamenti et al., 2015). The analysis revealed that acetate in *G. ferrihydriticus* could be produced from acetyl-CoA by the activity of phosphate acetyltransferase (Gfer_00485) and acetate kinase (Gfer_00490), while carbon dioxide could be fixed during the reversed citric acid cycle and completely encoded by the genome, including the main enzyme of the cycle: citrate lyase (Gfer_14125, Gfer_14130, Gfer_14140, Gfer_14145). Additionally, the enzymes of the methyl branch of the Wood-Ljungdahl pathway for CO_2 fixation was identified in the genome of *G. ferrihydriticus*. Acetyl-CoA from CO_2 fixation could be converted either into acetate as mentioned above or to pyruvate by pyruvate-ferredoxin oxidoreductase for further biosynthetic utilization in gluconeogenesis. Its genome encodes putative cation/acetate symporters, consistent with the ability of *G. ferrihydriticus* to utilize or produce acetate (Gfer_06630, Gfer_06625). Genome screening of *G. ferrihydriticus* for MtoABCD porin-cytochrome complex genes, which are used to determine Fe(II) oxidation in bacteria (Shi et al., 2014), retrieved homologs of MtoA putative outer membrane Fe(II)-oxidizing cytochrome, which is encoded by Gfer_00954, and MtoC inner membrane cytochrome with *c*-type and *b*-type domains, which are encoded by Gfer_00569. The MtoA homolog was predicted to possess a signal peptide and 17 heme-binding CXXCH motifs. A search for a chromosomal cassette that includes this gene with IMG/ER standard parameters revealed that Gfer_00954 clusters with two other *c*-type multihemes and two NHL-repeating proteins. Two multihemes of this cluster (Gfer_00956 and Gfer_00958) possessed signal peptides but shared no homology with typical periplasmic MtoD proteins. The homolog of the MtoC/CymA/MtrH quinone reducing protein was encoded in *G. ferrihydriticus* by Gfer_00569, which is clustered with the Na^+-translocating electron transfer complex RnfABCDEG genes and the F0F1-type ATP-synthase subunits Z, I, *a* and *c*. Other subunits of the ATP-synthase (ε, β, γ, α, δ and b) were encoded in a separate cluster: Gfer_00841–848. Sequence analysis of the *c* subunit did not allow us to reliably predict Na^+ translocation by this ATP-synthase, as only 2 of 5 previously described direct Na^+-coordinating residues, e.g., E65 and S66 in *Ilyobacter tartarticus* (Mulkidjanian et al., 2008), have been found in the atpC protein of *G. ferrihydriticus*.

4. Discussion

Despite many reports on dissimilatory iron reduction in alkaliphilic prokaryotes, the biological weathering mechanisms of iron-containing silicates have been extensively studied only under circumneutral conditions (see references in Uroz et al., 2009; Gadd, 2010; Konhauser et al., 2011; Melton et al., 2014). To our knowledge, only one work has addressed this topic (Liu et al., 2015), while Bethke et al. (2011) and Flynn et al. (2014) showed that iron reduction as a proton-consuming reaction is energetically unfavourable at alkaline pH, which does not seem to us to be adequately justified. Indeed, Na^+ ions might replace protons in extremely alkaline environments to overcome their scarcity and create an electron motive force that benefits certain alkaliphiles (Kevbrin et al., 1998; Krulwich et al., 2001; Detkova and Pusheva, 2006; Mulkidjanian et al., 2008). Additionally, most forms of iron oxides, carbonates and sulphides are stable at pH > 8.0 and low E_h (Garrels and Christ, 1965). From a thermodynamic point of view, microorganisms develop in the field of stability of their metabolic products and the field of metastability of substrates (Zavarzin, 1972); thus, alkaline conditions seem to favour DIRB because of the stability of magnetite and siderite, the main products of SF reduction. This observation could explain the common occurrence of iron-reducing alkaliphiles in soda lakes (Zavarzina et al., 2006). Iron-containing silicates are among the most abundant minerals in the Earth's crust and could serve as a common source of iron for DIRB in alkaline environments.

4.1. Bioweathering of phyllosilicates by Clostridium alkalicellulosi

In this work, we studied bioweathering that was caused by the activity of anaerobic microorganisms that represent two terminal groups of the alkaliphilic microbial trophic chain. *C. alkalicellulosi* is a cellulosolytic bacterium that is responsible for the first step of polysaccharide degradation and is a typical anaerobic fermentative bacterium that is incapable of respiration and the utilization of mixed valence elements as electron acceptors for energy generation (Zhilina et al., 2005). Possible interactions between *C. alkalicellulosi* and phyllosilicates are limited by the action of organic acids (formate, acetate, and lactate), which are formed as the main metabolic products of MCC degradation. The results of our studies confirmed that this weathering factor was not very significant under alkaline conditions. The solid phases, as analysed by different methods, showed an absence of changes in the biotite structure. Only FTIR analyses detected the appearance of a small amount of newly formed kaolinite, which indicated changes in the glauconite structure. This result could be explained by the differences between glauconite and biotite structures. The structure of glauconite is an intermediate structure between mica and smectite (nontronite). This structure contains less Al^{3+} and K^+ but more OH^- groups and thus exhibits some properties that are typical of swelling (smectite) minerals, e.g., enhanced cation exchange capacity (CEC). The CEC changes from 5 to 40 mg-eq/100 g depending on the percentage of swelling layers in the structure; for comparison, the CEC of biotite is around 10 mg-eq 100 g^{-1} (Minerals, 1992). The absence of detectable Si in the solutions in both the microbial cultures and sterile controls could be explained by silica sorption on MCC surfaces. Solubility measurements of pure solid phases that were separated from the culture medium reflected changes in the equilibrium concentration of dissolved silica and showed that microbial interaction with phyllosilicates was even lower than abiotic interaction (Table 4, first column bar in Fig. 1). This result could have been caused by mechanical barriers, such as the slime that *C. alkalicellulosi* forms during cellulose degradation, or by the production of extracellular microbial polysaccharides, which block reactive centres on minerals (Welch and Vandevivere, 1994; Welch et al., 1999). At the same time, an analysis of fermentation products that accumulated during MCC degradation by *C. alkalicellulosi* in the presence and absence of biotite or glauconite showed that the presence of these minerals changed the ratio of the products, inhibiting lactate production almost completely (Fig. 4). One possible explanation is that elements with mixed valence, including the components of phyllosilicates, acted as a sink for electrons that were released during fermentation. Thus, these elements from phyllosilicates decreased the production of reduced compounds and changed the ratios of metabolites that were formed during MCC degradation.

4.2. Bioweathering of phyllosilicates by Geoalkalibacter ferrihydriticus

The alkaliphilic dissimilatory iron-reducing bacterium *G. ferrihydriticus* exhibits only respiratory metabolism and grows through the reduction of different iron- and sulphur-containing compounds (Zavarzina et al., 2006). Microorganisms with this type of metabolism are responsible for the last stage of the anaerobic destruction of non-fermentable organic substrates, such as formate and acetate. Biotite and glauconite minerals, which contain ferric iron, could serve as electron

acceptors for *G. ferrihydriticus*. In this view, the increasing acetate concentration in the *G. ferrihydriticus* culture with minerals during the first days of our cultivation experiments is the most intriguing part of this work. We have previously observed the same phenomenon during SF reduction by the co-culture of *G. ferrihydriticus* and *Anaerobacillus alkalilacustris*, where acetate accumulated instead of being consumed (Zavarzina et al., 2011). Later, we demonstrated the ability of homoacetogenic alkaliphilic bacteria of the genus *Fuchsiella* to reduce Fe(III) during dissimilatory processes (Zhilina et al., 2015). Based on the results of this study, we propose the ability of *G. ferrihydriticus* to promote acetogenic growth on iron-containing phyllosilicates.

Solid phase analysis, including MS and Mössbauer spectroscopy (Chistyakova et al., 2012a, 2012b; Shapkin et al., 2013), clearly demonstrated that *G. ferrihydriticus* can utilize structural iron from biotite and glauconite lattices to form new magnetically ordered phases. Noticeably, the biotransformation of phyllosilicates resulted in magnetite formation during both bio-reduction and bio-oxidation. This result raises the following question: which valence state of iron was used by *G. ferrihydriticus* for the growth in our experiments? The presence of four quadrupole doublets on the Mössbauer spectra can be explained by different distribution of ferric and ferrous atoms in M1 (trans-octahedra) and M2 (*cis*-octahedra) sites, which have different positions of OH-groups (Govaert et al., 1979; Ali et al., 2001). The total intensities of the sub-spectra that correspond to Fe^{2+} and Fe^{3+} atoms (doublet) are shown in Fig. 3. Under the assumption that the recoil-less fractions (probability of Mössbauer effect) are equal for iron atoms that are located in different positions, the relative intensities of the relevant subspectra equal the relative amount of iron atoms in these positions. An analysis of the Mössbauer spectra showed that the formation of magnetically ordered phases was accompanied by solid-phase iron redistribution in the absence of an increase in the relative amount of Fe^{2+} atoms. On the other hand, the relative amount of all Fe^{3+} atoms increased in the experiments with *G. ferrihydriticus* (see the second and third column bars in Fig. 3). We have previously noted and explained this phenomenon by chemical iron oxidation (Shapkin et al., 2013). In this work, we registered an increase in the amount of Fe^{3+} atoms in the M1 and M2 sites of biotite in addition to the formation of magnetically ordered phases. An increase in Fe(III) for glauconite was also observed because the magnetically ordered phases contained at least 2/3 of the Fe^{3+} atoms. Thus, the formation of magnetically ordered phases in this experiment could be explained by Fe(II)-oxidation rather than by Fe(III)-reduction.

We propose the ability of *G. ferrihydriticus* to perform acetogenesis with Fe^{2+} as the electron donor and carbonate as the electron acceptor to explain the production of additional acetate and the decrease in Fe(II) instead of its expected increase. This assumption is supported by the results of genome analysis, which revealed possible genomic determinants of acetate production, CO_2 fixation and Fe(II) oxidation in *G. ferrihydriticus*. The most convincing predictions were those for acetate synthesis from acetyl-CoA by phosphate acetyltransferase and acetate kinase and for Fe(II) oxidation, which is supposed to be determined by the subunits of porin-cytochrome MtoABCD complexes (Shi et al., 2012; Liu et al., 2012). Genome analysis revealed the presence of outer membrane Fe(II)-oxidizing MtoA *c*-type multiheme cytochrome and inner membrane MtoC quinone-oxidizing cytochrome in *G. ferrihydriticus*. The first enzyme is encoded in a cluster with two other secreted cytochromes, which may serve as relays of electrons from MtoA to MtoC through the periplasmic space. The MtoC homolog mediates electron transfer between the quinone/quinol pool in the inner membrane and redox proteins in the periplasm. The *mtoC* gene in *G. ferrihydriticus* is clustered with the Rnf complex and F_0F_1-type ATP-synthase genes. Rnf complexes may act as an energy-conserving ferredoxin: NAD^+ oxidoreductase (Biegel and Muller, 2010; Biegel et al., 2011) couples the reduction of NAD^+ with the electrogenic pumping of Na^+ or H^+ ions across the membrane out of the cell. Na^+-pumping by the ATP-synthase of *G. ferrihydriticus* remains unclear, but several features of this enzyme that are specific to alkaliphiles could be derived from genome analysis. The ATP-synthase cluster in *G. ferrihydriticus* contains additional *atpI* and *atpZ* genes whose products have been shown to enhance the stability of the synthase and the ability to acquire sufficient magnesium in alkaliphiles (Preiss et al., 2015). The separation of the clusters that encode AtpZI*ac* and other subunits of the ATP-synthase, as observed in *G. ferrihydriticus*, has also been previously mentioned in the alkaliphile *Bacillus pseudofirmus* (Hicks et al., 2010). Generally, the major enzyme complexes in *G. ferrihydriticus* that are supposed to couple Fe(II) oxidation with energy generation are encoded in the same gene cluster.

We performed thermodynamic calculations for an experimental system with biotite to check the principal possibility of energy generation from Fe(II) oxidation under alkaline conditions. The results showed that biotite was a stable phase in equilibrium with high concentrations of acetate, which defined a reducing environment (Fig. 8). Iron was oxidized to magnetite, while the concentration of acetate increased from 12 to 17 mM. The acetate concentration in the experiments was lower than in the calculations because bacteria cannot reach chemical equilibrium. The acetate concentration is determined by mineral associations, so the acetate concentration increases at the beginning of the process and then decreases. The results of our thermodynamic calculations were strikingly similar to the experimental data. Accordingly, *G. ferrihydriticus* could produce acetate by Fe(II) oxidation under our experimental conditions.

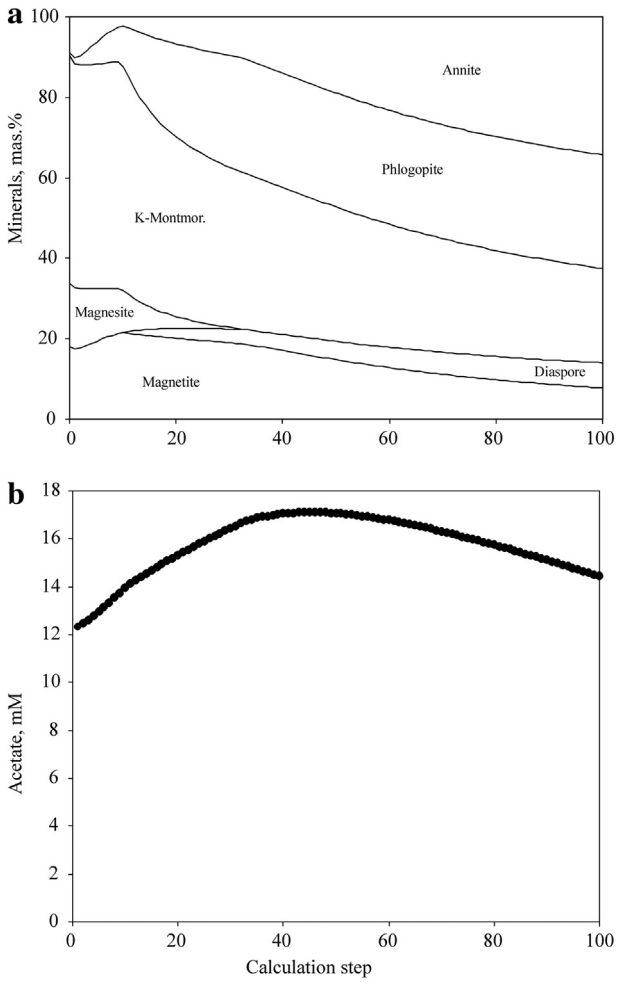

Fig. 8. Results of the thermodynamic calculations for an experimental system with biotite, which demostrate the possibility of simultaneous magnetite (a) and accetate (b) formation.

Table 3
Fermentation products that formed in the experiments (*Ex1–3*) and controls (*C2–3*) during bacterial growth and determination Fe(II) production.

Fe(II) and fermentation products, mM	Fe(II)		Formate		Acetate		Lactate		Ethanol	
Days\Duplicates	1	2	1	2	1	2	1	2	1	2
Ex1, biotite										
2			0.5	0.4	0.3	0.3	0.2	0.1	0.4	0.4
8			0.7	0.6	1.2	1.1	0.5	0.5	2.2	1.8
14			0.5	0.6	1.2	0.9	0.4	0.5	2.4	1.4
22			0.6	0.2	1.3	1.2	0.6	0.2	2.0	1.0
50			0.2	0.3	1.7	1.8	0.2	0.2	2.2	2.3
165			0.7	0.5	1.8	1.7	0.5	0.6	2.5	3.0
200			0.6	0.5	2.2	1.5	0.5	0.6	2.3	3.0
Ex1, glauconite										
2			0.5	0.6	0.3	0.3	0.2	0.1	0.4	0.2
8			0.7	0.7	1.2	1.2	0.5	0.6	1.4	2.2
14			0.6	0.7	1.0	1.2	0.5	0.6	2.1	2.5
22			0.7	0.8	1.3	1.4	0.5	0.7	1.5	2.3
50			0.5	0.6	0.9	1.3	0.5	0.6	1.8	3.0
165			0.7	0.6	1.3	1.3	0.7	0.6	3.2	3.1
200			0.6	0.7	1.3	1.3	0.6	0.7	3.1	3.3
Ex2, biotite										
2					11.9	9.3				
8					13.0	11.6				
14					13.4	13.6				
22					13.7	13.2				
50					13.5	11.9				
165					14.0	13.1				
200					14.1	13.2				
Ex2, glauconite										
2					9.9	9.5				
8					12.1	13.0				
14					12.0	13.8				
22					13.3	13.0				
50					11.5	12.2				
165					12.5	12.9				
200					12.1	13.0				
Ex3, biotite										
2			0.4	0.4	0.5	0.5	0.1	0.1	0.2	0.2
8			0.5	0.4	1.2	1.2	0.3	0.1	0.7	0.0
14			0.4	0.2	1.2	1.2	0.3	0.2	1.1	0.9
22			0.3	0.3	1.6	1.6	0.3	0.2	1.6	1.8
50			0.3	0.3	1.6	1.6	0.2	0.2	1.6	1.8
165			0.4	0.2	2.1	1.7	0.3	0.2	2.5	2.2
200			0.4	0.3	2.2	2.0	0.3	0.2	2.5	2.2
Ex3, glauconite										
2			0.3	0.3	0.4	0.5	0.1	0.1	0.2	0.2
8			0.0	0.3	1.2	1.2	0.2	0.2	1.1	0.9
14			0.1	0.3	0.5	1.2	0.1	0.2	0.2	0.8
22			0.4	0.3	2.0	2.0	0.2	0.3	1.0	1.3
50			0.4	0.2	2.1	2.0	0.2	0.2	2.2	2.0
165			0.4	0.0	2.0	2.6	0.2	0.2	2.3	2.2
200			0.4	0.0	2.0	2.6	0.2	0.2	2.2	2.0
C3, synthesized ferrihydrite										
2	2.6	3.5	0.0	0.0	0.5	0.5	0.0	0.0	0.0	0.0
8	8.5	9.4	0.3	0.4	1.9	2.0	0.2	0.2	0.9	0.0
14	13.3	12.9	0.2	0.2	2.1	2.6	0.1	0.1	0.8	0.5
22	10.3	11.6	0.3	0.2	2.6	3.4	0.2	0.2	0.8	1.0
50	13.5	15.9	0.1	0.0	2.9	4.6	0.1	0.1	1.3	0.7
165	14.6	16.7	0.0	0.0	3.2	5.9	0.3	0.1	0.4	0.0
200	13.8	15.3	0.0	0.0	3.3	5.5	0.2	0.1	0.2	0.0
C23										
2			0.3	0.5	0.1	0.2	0.2	0.3	0.1	0.2
8			0.5	0.5	0.9	0.7	2.3	1.8	1.1	1.5
14			0.5	0.5	1.1	1.0	2.5	2.1	1.9	1.5
22			0.5	0.5	1.0	1.1	2.4	2.1	1.5	1.6
50			0.4	0.4	0.9	0.9	2.3	1.9	2.0	1.9
165			0.4	0.4	1.0	0.9	2.4	1.8	2.2	1.7
200			0.5	0.5	1.0	1.0	2.6	2.2	2.0	2.2

Table 4
Data of Si that dissolved from phyllosilicates during bacterial growth and magnetic susceptibility.

Experiments	Duplicates	Si, μM		MS, $\times 10^{-8}$ m^3 kg^{-1}	
		Biotite	Glauconite	Biotite	Glauconite
Ex1	1	27.1	60.4	314	53
	2	30.4	70.0	324	65
Ex2	1	98.1	91.0	4191	7062
	2	97.4	84.8	6978	6217
Ex3	1	78.7	79.9	7595	7460
	2	72.5	87.3	7248	15321
C1		34.6	73.9	360	85

When compared to the results from the sterile controls (*C1*) and the experiment with *C. alkalicellulosi* (*Ex1*), the influence of *G. ferrihydriticus* on biotite caused a three-fold increase in the dissolved Si concentration, while the difference for glauconite was only 40%. However, glauconite contains three times less ferrous iron than biotite (Table 1). The formation of new phases from the oxidation of ferrous iron can explain why the dissolved Si concentration was much less for glauconite than for biotite: the concentration of dissolved silica directly depends on the amount of ferrous iron that is oxidized by *G. ferrihydriticus*. When the cells of *G. ferrihydriticus* attack Fe^{2+} atoms in the octahedral layers of biotite and glauconite and remove them from the crystal lattice, the silicate lattice structure collapses, increasing the dissolved Si concentration.

4.3. Growth of *Clostridium alkalicellulosi* and *Geoalkalibacter ferrihydriticus* in co-cultures

A binary culture of *C. alklalicellulosi* and *G. ferrihydriticus* reproduces the simplest trophic chain of anaerobic destructors, performing the complete mineralization of organic matter (e.g., MCC). Our results in the control experiment with SF as the electron acceptor showed that this trophic chain works. We observed a stepwise decrease in formate and ethanol that was utilized by *G. ferrihydriticus* as electron donors concomitantly with acetate accumulation and SF reduction to magnetite and siderite. These data are in complete agreement with our previous results (Zavarzina et al., 2011) and demonstrate that *G. ferrihydriticus* growth does not depend on the fermentative partner. The increase in the acetate concentration during the entire incubation period could be explained by its production by *G. ferrihydriticus* during the oxidation of ethanol according to the following reaction:

$$C_2H_5OH + 4Fe^{3+} + H_2O = CH_3COO^- + 4Fe^{2+} + 5H^+.$$

The oxidation of ethanol began on the 50th day of the experiment after the exhaustion of formate. Approximately 1 mM of ethanol was oxidized during the last 150 days of the experiment, which correspondingly increased the acetate content during this period.

The results of silicate bioweathering by a binary culture of *G. ferrihydriticus* and *C. alklalicellulosi* were almost completely identical to those of a *G. ferrihydriticus* monoculture. An analysis of the Mössbauer spectra revealed that magnetically ordered phases was formed when biotite was used because of the oxidation of Fe^{2+} (Table 5, third column bar in Fig. 3a). Moreover, the relative amount of ferric iron in the biotite structure increased by up to 5% compared to the sterile control (*C1*). The data for glauconite were not so clear (Table 5, third column bar in Fig. 3b). The summarized ratio between Fe^{3+} and Fe^{2+} before and after the experiment remained almost unchanged. However, the Mössbauer spectroscopy data did not allow us to determine how much magnetite or maghemite had been formed. The very similar Si equilibrium concentrations as those in *Ex2* (Table 4, Fig. 1) indicate that the mechanism of *G. ferrihydriticus* action on biotite and glauconite in both experiments was similar.

Table 5
Relative intensities of sub-spectra that correspond to ferric and ferrous ions and the magnetically ordered phases in biotite (Ali et al., 2001) and glauconite (Anbar et al., 2007).

Experiments	Fe^{3+} (M1), %		Fe^{3+} (M2), %		Fe^{2+} (M1), %		Fe^{2+} (M2), %		Magnetically ordered phase, %	
	1	2	1	2	1	2	1	2	1	2
Ex1	9.4 ± 0.1	51.0 ± 3.4	9.4 ± 0.2	24.3 ± 3.4	62.6 ± 0.9	14.5 ± 2.8	18.7 ± 0.8	10.3 ± 2.5	0	0
Ex2	9.8 ± 0.2	39.3 ± 4.2	9.7 ± 0.2	23.7 ± 3.9	59.0 ± 0.9	10.6 ± 0.8	10.8 ± 0.4	10.2 ± 0.7	10.7 ± 1.3	16.2 ± 1.9
Ex3	11.8 ± 0.3	17.1 ± 1.1	11.8 ± 0.3	45.0 ± 1.1	53.5 ± 1.4	9.4 ± 0.3	13.3 ± 0.7	7.1 ± 0.3	10.1 ± 2.0	21.5 ± 0.8
C1	8.8 ± 0.2	47.0 ± 1.7	8.7 ± 0.2	28.9 ± 1.8	64.4 ± 0.8	14.6 ± 2.4	18.1 ± 0.7	9.5 ± 2.2	0	0

5. Conclusions

The above experiments allowed us to draw the following conclusions:

- Alkaliphilic bacteria significantly influenced the bioweathering of iron-containing phyllosilicate minerals. *C. alkalicellulosi* changed the structure of glauconite and participated in the neoformation of kaolinite.
- The presence of biotite and glauconite in the culture medium directly influenced the ratios of metabolic products that were formed by *C. alkalicellulosi* and repressed lactate production.
- *G. ferrihydriticus*, both alone and in a co-culture with *C. alkalicellulosi*, transformed biotite and glauconite with the formation of a novel magnetically ordered mineral phase, which represented a mixture of non-stoichiometric magnetite and maghemite. To our knowledge, this study is the first report on the ability of DIRB to use iron from glauconite during its catabolism.
- The increasing acetate concentration in the experiments with pure cultures of *G. ferrihydriticus* that grew on phyllosilicates could be explained by the oxidation of Fe(II) from biotite or glauconite to Fe(III), with carbonate being the electron donor. This hypothesis is supported by the results of Mössbauer spectroscopy, genome analysis of *G. ferrihydriticus* and thermodynamic calculations, thus revealing the ability of the organism to perform acetogenesis coupled with Fe(II) oxidation.

6. Geological applications

The unexpected results of this research allow us to make some geological speculations. The source of iron for banded iron formations (BIF) during almost the entire late Archean (2.7–2.4 Ga) is agreed to have been Fe(II) (Trendall, 2002; Klein, 2005). The presence of Fe(III) minerals in BIFs dictates that some form of Fe(II)-oxidizing mechanism(s) was necessary for their formation (Posth et al., 2013). Because the Great Oxygenation Event occurred at approximately 2.5 Ga (Anbar et al., 2007), an alternative, O_2-independent mechanism is proposed to explain the deposition of the earliest BIFs. The participation of microorganisms in BIF deposition was first proposed by Cloud (1968). The presence of ferric iron minerals in banded iron formations (BIF) is generally accepted to have been caused by the metabolic activity of planktonic bacteria in the oceanic photic zone (Johnson et al., 2008; Konhauser et al., 2011; Li et al., 2011; Posth et al., 2013). Two biological processes that may cause the anaerobic oxidation of iron are known to be driven by microorganisms: (i) photosynthetic Fe(II) oxidation (Widdel et al., 1993) and (ii) nitrate reduction that is coupled with iron(II) oxidation (Straub et al., 1996; Zhao et al., 2013; Zhao et al., 2015). Both of these reactions have some limitations in relation to the Precambrian conditions of BIF deposition. Photoferrotrophic microorganisms face a problem in the limited availability of dissolved Fe(II) and require very special surface habitats to receive light and, on the other hand, to access ferrous iron. Nitrate-dependent Fe(II)-oxidizing bacteria require the presence of nitrates, which is unlikely in anoxic environments, and strongly depend on organic substrates (Konhauser et al., 2011). If our suggestion on the ability of *G. ferrihydriticus* to oxidize ferrous iron with carbonate as an electron acceptor is correct, this biological process could have played a significant role in ancient environments. The growth of such microorganisms would not be limited by the availability of the energy source or the electron acceptor in the Archaean biosphere; thus, these microorganisms could have acted as efficient primary producers of organic matter.

Several hypotheses have postulated that alkaline conditions may have predominated in large areas of the Precambrian ocean (termed a soda ocean) (Kempe and Degens, 1985; Kempe et al., 1989), the Precambrian continent (termed soda continent) (Zavarzin, 1993) and even the subsurface of Europa (Kempe and Kazmierczak, 2002). Some evidence exists of continental alkaline lakes during the Archean (Stueeken et al., 2015). High-temperature hydrothermal fluids in the Archean sub-seafloor basalt-hosted hydrothermal system were likely highly alkaline, unlike modern conditions (Shibuya et al., 2010). The existence of a soda ocean seems doubtful, but the appearance of large shallow Magadi lake-like ponds on the Precambrian continents is highly probable because the environmental conditions of the ancient continents favoured such formations for the following reasons: (i) a lack of plants and soil to contribute to the weathering of igneous rocks and smooth out the relief; (ii) carbon dioxide partial pressure that was not below but rather above the present values; (iii) the atmospheric hydrological cycle that formed during the early stages of Earth's history; and (iv) the higher temperature on the Earth's surface, which contributed to the rapid evaporation of water and concentration of salts in drainage areas. In such ponds, where the sulphur cycle did not occur because of the absence of sulphates, microorganisms such as *G. ferrihydriticus* could play a central role in microbial communities because of their ability to couple both iron reduction and oxidation with acetate production.

Acknowledgements

We would like to thank Dr. E.A. Bonch-Osmolovskaya and Dr. V.S. Savenko for their helpful discussion and interest in our work and Dr. A.O. Alekseev for the MS measurements. This work was supported by the RFBR's research projects No 14-05-00345 and 13-04-40205H and by research program No 30 of the Presidium of RAS: "The origin of life and evolution of geo-biological systems". The thermodynamic analysis in this work was supported by RSF project No. 14-50-00029.

References

Ali, A.M., Hsia, Y., Liu, R., Zhang, J., Duan, W., Chen, L., 2001. A Mössbauer study of evolution of glauconite from Chinese seas. Spectrosc. Lett. 34, 701–708.
Anbar, A.D., Duan, Y., Lyons, T.W., Arnold, G.L., Kendall, B., Creaser, R.A., Kaufman, A.J., Gordon, G.W., Scott, C., Garvin, J., Buick, R., 2007. A whiff of oxygen before the Great Oxidation Event? Science 317, 1903–1906.
Badalamenti, J.P., Krajmalnik-Brown, R., Torres, C.I., Bond, D.R., 2015. Genomes of *Geoalkalibacter ferrihydriticus* Z-0531^T and *Geoalkalibacter subterraneus* Red1^T, two haloalkaliphilic metal-reducing *Deltaproteobacteria*. Genome Announc. 3 (2), e00039-15.
Banfield, J.F., Nealson, K.H., 1998. Geomicrobiology: Interactions between Microbes and Minerals. Mineralogical Society of America, Washington, DC [Reviews in Mineralogy No. 35.].
Bethke, C.M., Sanford, R.A., Kirk, M.F., Jin, Q., Flynn, T.M., 2011. The thermodynamic ladder in geomicrobiology. Am. J. Sci. 311, 183–210.
Biegel, E., Muller, V., 2010. Bacterial Na^+-translocating ferredoxin: NAD^+ oxidoreductase. Proc. Natl. Acad. Sci. U. S. A. 107, 18138–18142.

Biegel, E., Schmidt, S., Gonzalez, J.M., Muller, V., 2011. Biochemistry, evolution and physiological function of the Rnf complex, a novel ion-motive electron transport complex in prokaryotes. Cell. Mol. Life Sci. 68, 613–634.

Bond, D.R., Lovley, D.R., 2002. Reduction of Fe(III) oxide by methanogens in the presence and absence of extracellular quinones. Environ. Microbiol. 4, 115–124.

Brookshaw, D.R., Coker, V.S., Lloyd, J.R., Vaughan, D.J., Pattrick, R.A.D., 2015. Redox interactions between Cr(VI) and Fe(II) in bioreduced biotite and chlorite. Environ. Sci. Technol. http://dx.doi.org/10.1021/es5031849.

Brookshaw, D.R., Lloyd, J.R., Vaughan, D.J., Pattrick, R.A.D., 2014. Bioreduction of biotite and chlorite by a *Shewanella* species. Am. Mineral. 99, 1746–1754.

Chistyakova, N.I., Rusakov, V.S., Shapkin, A.A., Pigalev, P.A., Kazakov, A.P., Zhilina, T.N., Zavarzina, D.G., Lančok, A., Kohout, J., Greneche, J.-M., 2012a. Mössbauer and magnetic study of solid phases formed by dissimilatory iron-reducing bacteria. Solid State Phenom. 190, 721–724.

Chistyakova, N.I., Rusakov, V.S., Shapkin, A.A., Zhilina, T.N., D.G., Z., 2012b. Mössbauer study of dissimilatory reduction of iron contained in glauconite by alkaliphilic bacteria. Hyperfine Interact. 208, 85–89.

Cloud, P., 1968. Atmospheric and hydrospheric evolution on the primitive earth. Science 160, 729–736.

Coupland, K., Johnson, D.B., 2008. Evidence that the potential for dissimilatory ferric iron reduction is widespread among acidophilic heterotrophic bacteria. FEMS Microbiol. Lett. 279, 30–35.

Detkova, E.N., Pusheva, M.A., 2006. Energy metabolism in halophilic and alkaliphilic acetogenic bacteria. Microbiology (English translation of Mikrobiologiya) 75, 1–11.

Dong, H., 2012. Clay–microbe interactions and implications for environmental mitigation. Elements 8, 113–118.

Dong, H., Kukkadapu, R.K., Fredrickson, J.K., Zachara, J.M., Kennedy, D.W., Kostandarithes, H.M., 2003. Microbial reduction of structural Fe(III) in illite and goethite. Environ. Sci. Technol. 37, 1268–1276.

Ehrlich, H.L., 1998. Geomicrobiology: Its significance for geology. Earth Sci. Rev. 45, 45–60.

Eugster, H.P., Hardie, L.A., 1978. Saline lakes. In: Lerman, A. (Ed.), Lakes — Chemistry, Geology, Physics. Springer Verlag, N.Y., pp. 237–293.

Ferris, F.G., Wiese, R.G., Fyfe, W.S., 1994. Precipitation of carbonate minerals by microorganisms: implications for silicate weathering and the global carbon dioxide budget. Geomicrobiol J. 12, 1–13.

Flynn, T.M., O'Loughlin, E.J., Mishra, B., DiChristina, T.J., Kemner, K.M., 2014. Sulfur-mediated electron shuttling during bacteria iron reduction. Science 344 (6187), 1039–1042.

Gadd, G.M., 2010. Metals, minerals and microbes: geomicrobiology and bioremediation. Microbiology 156, 609–643.

Gadd, G.M., Sayer, G.M., 2000. Fungal transformations of metals and metalloids. In: Lovley, D.R. (Ed.), Environmental Microbe Metal Interactions. American Society for Microbiology, Washington, DC, pp. 237–256.

Garrels, R.M., Christ, C.L., 1965. Solutions, Minerals and Equilibria. Harper and Row, New York.

Gorlenko, V., Tsapin, A., Namsaraev, Z., Teal, T., Tourova, T., Engler, D., Mielke, R., Nealson, K., 2004. *Anaerobranca californiensis* sp. nov., an anaerobic, alkalithermophilic, fermentative bacterium isolated from a hot spring on Mono Lake. IJSEM 54, 739–743.

Govaert, A., de Grave, E., Quartier, H., Chambaere, D., Robbrecht, G., 1979. Mössbauer analysis of glauconites of different belgian finding places. J. Phys. 40, 442–444.

Goya, G.F., Berquo, T.S., Fonseca, F.C., et al., 2003. Static and dynamic magnetic properties of spherical magnetite nanoparticles. J. Appl. Physiol. 94, 3520–3528.

Grote, G., Krumbein, W.E., 1992. Microbial precipitation of manganese by bacteria and fungi from desert rock and rock varnish. Geomicrobiol J. 10, 49–57.

Hicks, D.B., Liu, J., Fujisawa, M., Krulwich, T.A., 2010. F1F0-ATP synthases of alkaliphilic bacteria: lessons from their adaptations. Biochim. Biophys. Acta 1797, 1362–1377.

Hutchens, E., 2009. Microbial selectivity on mineral surfaces: Possible implications for weathering processes. Fungal Biol. Rev. 23, 115–121.

Johnson, C., Beard, B.L., Klein, C., Beukes, N.J., Roden, E.E., 2008. Iron isotopes constrain biologic and abiologic processes in banded iron formation genesis. Geochim. et Cosmochim. Acta 72, 151–169.

Jones, D.H., Srivastava, K.K.P., 1986. Many-state relaxation model for Mössbauer spectra of superparamagnets. Phys. Rev. B 34, 7542–7548.

Kalinowski, B.E., Liermann, L.J., Givens, S., Brantley, S.L., 2000. Rates of bacteria-promoted solubilization of Fe from minerals: a review of problems and approaches. Chem. Geol. 169, 357–370.

Kempe, S., Degens, E.T., 1985. An early soda ocean? Chem. Geol. 53, 95–108.

Kempe, S., Kazmierczak, J., 2002. Biogenesis and early life on earth and Europa: favored by an alkaline ocean? Astrobiology 2, 123–130.

Kempe, S., Kazmierczak, J., Degens, E.T., 1989. The soda ocean concept and its bearing on biotic evolution. In: Crick, R.E. (Ed.), Origin, Evolution and Modern Aspects of Biomineralization in Plants and Animals. Plenum Press, N.Y., pp. 29–39.

Kevbrin, V.V., Zavarzin, G.A., 1992. The effect of sulfur compounds on growth of halophilic the homoacetic bacterium *Acetohalobium arabaticum*. Microbiology (English translation of Mikrobiologiya) 61, 812–817.

Kevbrin, V.V., Zhilina, T.N., Rainey, F.A., Zavarzin, G.A., 1998. *Tindallia magadii* gen. Nov., sp. nov.: an alkaliphilic anaerobic ammonifier from soda lake deposits. Curr. Microbiol. 37, 94–100.

Klein, C., 2005. Some Precambrian banded iron formations (BIFs) from around the world. Their age, geologic setting, mineralogy, metamorphism, geochemistry,and origin. Am. Mineral. 90, 1473–1499.

Konhauser, K.O., Kappler, A., Roden, E.E., 2011. Iron in microbial metabolism. Elements 7, 89–93.

Koo, T., Jang, Y., Kogure, T., Kim, J.H., Park, B.C., Sunwoo, D., Kim, J., 2014. Structural and chemical modification of nontronite associated with microbial Fe(III) reduction: indicators of "illitization". Chem. Geol. 377, 87–95.

Kraemer, S.M., Cheah, S.F., Zapf, R., Xu, J.D., Raymond, K.N., Sposito, G., 1999. Effect of hydroxamate siderophores on Fe release and Pb(II) adsorption by goethite. Geochim. Cosmochim. Acta 63, 3003–3008.

Krulwich, T.A., Ito, M., Guffanti, A.A., 2001. The Na^+-dependence of alkaliphily in *Bacillus*. Biochim. Biophys. Acta Bioenerg. 1505, 158–168.

Li, Y., Konhauser, K.O., Cole, D.R., Phelps, T.J., 2011. Mineral ecophysiological data provide growing evidence for microbial activity in banded-iron formations. Geology 39, 707–710.

Liermann, L.J., Kalinowski, B.E., Brantley, S.L., Ferry, J.G., 2000. Role of bacterial siderophores in dissolution of hornblende. Geochim. Cosmochim. Acta 64, 587–602.

Liu, D., Dong, H., Wang, H., Zhao, L., 2015. Low-temperature feldspar and illite formation through bioreduction of Fe(III)-bearing smectite by an alkaliphilic bacterium. Chem. Geol. 406, 25–33.

Liu, D., Dong, H., Zhao, L., Wang, H., 2014. Smectite reduction by *Shewanella* species as facilitated by cystine and cysteine. Geomicrobiol J. 31, 53–63.

Liu, J., Wang, Z., Belchik, S.M., Edwards, M.J., Liu, C., Kennedy, D.W., et al., 2012. Identification and characterization of MtoA: a decaheme c-type cytochrome of the neutrophilic Fe(II)-oxidizing bacterium *Sideroxydans lithotrophicus* ES-1. Front. Microbiol. 3, 37.

Lovley, D.R., Phillips, E.J.P., 1988. Novel mode of microbial energy metabolism: organic carbon oxidation coupled to dissimilatory reduction of iron or manganese. Appl. Environ. Microbiol. 54, 1472–1480.

Lovley, D.R., Holmes, D.E., Nevin, K.P., 2004. Dissimilatory Fe(III) and Mn(IV) reduction. Adv. Microb. Physiol. 49, 219–286.

Lur'e, Y., 1971. Unified Methods of Water Analysis. Khimiya, Moscow (in Russian).

Ma, C., Zhuang, L., Zhou, S.G., Yang, G.Q., Yuan, Y., Xu, R.X., 2012. Alkaline extracellular reduction: isolation and characterization of an alkaliphilic and halotolerant bacterium, *Bacillus pseudofirmus* MC02. J. Appl. Microbiol. 112, 883–891.

Manghnani, M.H., Hower, J., 1964. Glauconites: cation exchange capacities and infrared spectra. Part II. Infrared absorption characteristics of glauconites. Am. Mineral. 49, 1631–1642.

Matsnev, M.E., Rusakov, V.S., 2014. Study of spatial spin-modulated structures by Mössbauer spectroscopy using SpectrRelax. AIP Conf. Proc. 1622, 40–49.

Melton, E.D., Swanner, E.D., Behrens, S., Schmidt, C., Kappler, A., 2014. The interplay of microbially mediated and abiotic reactions in the biogeochemical Fe cycle. Nat. Rev. Microbiol. 12, 797–808.

Mineraly, Spravochnik (in Russian) (1992). Ed. F.V. Chuhrov, Nauka, Moscow, Volume IV, (662 p).

Mulkidjanian, A.Y., Dibrov, P., Galperin, M.Y., 2008. The past and present of sodium energetics: may the sodium-motive force be with you. Biochim. Biophys. Acta 1777, 985–992.

O'Loughlin, E.J., Gorski, C.A., Scherer, M.M., Boyanov, M.I., Kemner, K.M., 2010. Effects of oxyanions, natural organic matter, and bacterial cell numbers on the bioreduction of lepidocrocite (γ-FeOOH) and the formation of secondary mineralization products. Environ. Sci. Technol. 44, 4570–4576.

Pentrakova, L., Su, K., Pentrak, M., Stucki, J.W., 2013. A review of microbial redox interactions with structural Fe in clay minerals. Clay Miner. 48, 543–560.

Pollock, J.P., Weber, K.A., Lack, J., Achenbach, L.A., Mormile, M.R., Coates, J.D., 2007. Alkaline iron(III) reduction by a novel alkaliphilic, halotolerant, *Bacillus* sp. isolated from salt at sediments of Soap Lake. Appl. Microbiol. Biotechnol. 77, 927–934.

Posth, N.R., Inga, K.I., Swanner, E.D., Schröder, C., Wellmann, E., Binder, B., Konhauser, K.O., Udo, N.U., Berthold, C., Nowak, M., Kappler, A., 2013. Simulating Precambrian banded iron formation diagenesis. Chem. Geol. 362, 66–73.

Preiss, L., Hicks, D.B., Suzuki, S., Meier, T., Krulwich, T.A., 2015. Alkaliphilic bacteria with impact on industrial applications, concepts of early life forms, and bioenergetics of ATP synthesis. Front. Bioeng. Biotechnol. 3, 75. http://dx.doi.org/10.3389/fbioe.2015.00075.

Richter, K., Schicklberger, M., Gescher, J., 2012. Dissimilatory reduction of extracellular electron acceptors in anaerobic respiration. Appl. Environ. Microbiol. 78, 913–921.

Roh, Y., Gao, H., Vali, H., Kennedy, D.W., Yang, Z.K., Gao, W., Dohnalkova, A.C., Stapleton, R.D., Moon, J., Phelps, T.J., Fredrickson, J.K., Zhou, J., 2006. Metal reduction and iron biomineralization by a psychrotolerant Fe(III)-reducing bacterium, *Shewanella* sp. strain PV-4. Appl. Environ. Microbiol. 72, 3236–3244.

Shapkin, A.A., Chistyakova, N.I., Rusakov, V.S., Zhilina, T.N., Zavarzina, D.G., 2013. Mössbauer study of bacterial iron-reduction processes in natural glaukonite and biotite. Bull. Russ. Acad. Sci. Phys. 77, 734–738.

Shi, L., Fredrickson, J.K., Zachara, J.M., 2014. Genomic analyses of bacterial porin-cytochrome gene clusters. Front. Microbiol. http://dx.doi.org/10.3389/fmicb.2014.00657.

Shi, L., Rosso, K.M., Zachara, J.M., Fredrickson, J.K., 2012. Mtr extracellular electron-transfer pathways in Fe(III)-reducing or Fe(II)-oxidizing bacteria: a genomic perspective. Biochem. Soc. Trans. 40, 1261–1267.

Shi, L., Squier, T.C., Zachara, J.M., Fredrickson, J.K., 2007. Respiration of metal (hydr)oxides by *Shewanella* and *Geobacter* a key role for multihaem *c*-type cytochromes. Mol. Microbiol. 65, 12–20.

Shibuya, T., Komiya, T., Nakamura, K., Takai, K., Maruyamad, S., 2010. Highly alkaline, high-temperature hydrothermal fluids in the early Archean ocean. Precam. Res. 182, 230–238.

Shvarov, Y., 2015. A suote of programs, OptimA, OptimB, OptimC and OptimS compatible with the Unitherm database, for deriving the thermodynamic properties of aqueous species from solubility, potentiometry and spectroscopy measurements. Appl. Geochem. 55, 17–27.

Slobodkin, A.I., 2005. Thermophilic microbial metal reduction. Microbiology (English translation of Mikrobiologiya) 74, 501–514.

Stookey, L.L., 1970. Ferrozine - a new spectrophotometric reagent for iron. Anal. Chem. 42, 779–781.

Straub, K.L., Benz, M., Schink, B., Widdel, F., 1996. Anaerobic, nitrate-dependent microbial oxidation of ferrous iron. Appl. Environ. Microbiol. 62, 1458–1460.

Stueeken, E.E., Buick, R., Schauer, A.J., 2015. Nitrogen isotope evidence for alkaline lakes on late Archean continents. Earth Planet. Sci. Lett. 411, 1–10.
Trendall, A.F., 2002. The significance of iron-formation in the Precambrian stratigraphic record. Int. Assoc. Sedimentol. Spec. Publ. 33, 33–66.
Uroz, S., Calvaruso, C., Turpault, M.-P., Frey-Klett, P., 2009. The microbial weathering of soil minerals, ecology, actors and mechanisms. Trends Microbiol. 17, 378–387.
Van Cappellen, P., Wang, Y., 1996. Cycling of iron and manganese in surface sediments: a general theory for the coupled transport and reaction of carbon, oxygen, nitrogen, sulfur, iron and manganese. Am. J. Sci. 296, 197–243.
Vaughan, D.J., Pattrick, R.A.D., Wogelius, R.A., 2002. Minerals, metalsand molecules: ore and environmental mineralogy in the new millenium. Mineral. Mag. 66, 653–676.
Welch, S.A., Vandevivere, P., 1994. Effect of microbial and other naturally occurring polymers on mineral dissolution. Geomicrobiol J. 12, 227–238.
Welch, S.A., Barker, W.W., Banfield, J.F., 1999. Microbial extracellular polysaccharides and plagioclase dissolution. Geochim. Cosmochim. Acta 63, 1405–1419.
Widdel, F., Schnell, S., Heising, S., Ehrenreich, A., Assmus, B., Schink, B., 1993. Ferrous iron oxidation by anoxygenic phototrophic bacteria. Nature 362, 834–836.
Zachara, J.M., Fredrickson, J.K., Li, S.W., Kennedy, D.W., Smith, S.C., Gassman, P.L., 1998. Bacterial reduction of crystalline Fe(III) oxides in single phase suspensions and subsurface materials. Am. Mineral. 83, 1426–1443.
Zachara, J.M., Kukkadapu, R.K., Fredrickson, J.K., Gorby, Y.A., Smith, S.C., 2002. Biomineralization of poorly crystalline Fe(III) oxides by dissimilatory metal reducing bacteria (DMRB). Geomicrobiol J. 19, 179–207.
Zavarzin, G.A., 1972. The Lithotrophyc Microorganisms. Nauka, Moscow (in Russian).
Zavarzin, G.A., 1993. Epicontinental soda lakes are probable relict biotopes of terrestrial biota formation. Microbiology (English translation of Mikrobiologiya) 62, 473–479.
Zavarzin, G.A., Zhilina, T.N., 2000. Anaerobic chemotrophic alkaliphiles. In: Seckbach, J. (Ed.), Journey to Diverse Microbial Worlds — Adaptation to Exotic Environments. Kluwer Academic Publishers, Netherlands, pp. 191–208.
Zavarzina, D.G., Kevbrin, V.V., Zhilina, T.N., Chystyakova, N.I., Shapkin, A.A., Zavarzin, G.A., 2011. Reduction of synthetic ferrihydrite by a binary anaerobic culture of *Anaerobacillus alkalilacustris* and *Geoalkalibacter ferrihydriticus* grown on mannitol at pH 9.5. Microbiology (English translation of Mikrobiologiya) 80, 743–757.
Zavarzina, D.G., Kolganova, T.V., Bouligina, E.S., Kostrikina, N.A., Tourova, T.P., Zavarzin, G.A., 2006. *Geoalkalibacter ferrihydriticus* gen. nov., sp. nov., the first alkaliphilic representative of the family *Geobacteraceae*, isolated from a soda lake. Microbiology (English translation of Mikrobiologiya) 78, 723–731.
Zavarzina, D.G., Pchelintseva, N.F., Zhilina, T.N., 1996. Calcium leaching by primary anaerobes. Microbiology (English translation of Mikrobiologiya) 65, 604–608.
Zhang, J., Dong, H., Liu, D., Agrawal, A., 2013. Microbial reduction of Fe(III) in smectite minerals by thermophilic methanogen *Methanothermobacter thermautotrophicus*. Geochim. Cosmoch. Acta 106, 203–215.
Zhao, L., Dong, H., Kukkadapu, R., Agrawal, A., Liu, D., Zhang, J., R.E., E., 2013. Biological oxidation of Fe(II) in reduced nontronite coupled with nitrate reduction by *Pseudogulbenkiania* sp. strain 2002. Geochim. Cosmochim. Acta 119, 231–247.
Zhao, L., Dong, H., Kukkadapu, R.K., Zeng, Q., Edelmann, R.E., Pentrak, M., Agrawal, A., 2015. Biological redox cycling of iron in nontronite and its potential application in nitrate removal. Environ. Sci. Technol. 49, 5493–5501.
Zhilina, T.N., Zavarzina, D.G., Kolganova, T.V., Lysenko, A.M., Tourova, T.P., 2009a. *Alkaliphilus peptidofermentans* sp. nov., a new alkaliphilic bacteria soda lake isolate capable of peptide fermentation and Fe(III) reduction. Microbiology (English translation of Mikrobiologiya) 78, 445–454.
Zhilina, T.N., Zavarzina, D.G., Osipov, G.A., Kostrikina, N.A., Tourova, T.P., 2009b. *Natronincola ferrireducens* sp. nov., and *Natronincola peptidivorans* sp. nov., new anaerobic, alkaliphilic, peptolytic iron-reducing bacteria isolated from soda lake. Microbiology (English translation of Mikrobiologiya) 78, 455–467.
Zhilina, T.N., Kevbrin, V.V., Tourova, T.P., Lysenko, A.M., Kostrikina, N.A., Zavarzin, G.A., 2005. *Clostridium alkalicellum* sp. nov., an obligately alkaliphilic cellulolytic bacterium from a soda lake in the Baikal region. Microbiology (English translation of Mikrobiologiya) 74, 557–566.
Zhilina, T.N., Zavarzina, D.G., Detkova, E.N., Patutina, E.O., Kuznetsov, B.B., 2015. *Fuchsiella ferrireducens* sp. nov., a novel haloalkaliphilic, lithoautitrophic homoacetogen capable of iron reduction, and emendation of the description of the genus *Fuchsiella*. IJSEM 65, 2432–2440.